

# Chapter 3

## Iris Pattern Recognition with a New Mathematical Model to Its Rotation Detection

Krzysztof Misztal, Emil Saeed, Jacek Tabor, and Khalid Saeed

**Abstract** The work deals with the iris pattern recognition as one of the most popular automated biometric ways of individual identification. It is based on the acquired eye images in which we localize the region of interest – the iris. This extremely data-rich biometric identifier is stable throughout human life and well protected as internal part of the eye. Moreover, it is genetic independent, so that we can use it to identify or verify people among huge population. This chapter will present the human vision nature focusing on defects and diseases that change the surface information of the iris. Also will be shown the main stream and the historical background of mathematical research resulting in a new algorithm for automatic iris feature extraction. A special attention is paid to the method developed to detect the iris rotation for accurate success rate under different destructive problems and environmental conditions. The obtained results after using the new mathematical model have proved the algorithm high success rate in iris pattern recognition.

---

K. Misztal (✉)

AGH University of Science and Technology, Kraków, Poland

e-mail: [krzysztof.misztal@gmail.com](mailto:krzysztof.misztal@gmail.com)

E. Saeed

Medical University in Białystok, Białystok, Poland

J. Tabor

Jagiellonian University, Kraków, Poland

K. Saeed

AGH University of Science and Technology, Faculty of Physics and Applied

Computer Science, Al. Mickiewicza 30, Kraków PL-30059, Poland

e-mail: [saeed@agh.edu.pl](mailto:saeed@agh.edu.pl)

### 3.1 History of Iris Recognition

The idea of using iris patterns for personal identification is very old [1]. However, the idea of automating this process was originally suggested in 1936 by ophthalmologist Frank Burch. In 1987 two American ophthalmologists, Aran Safir and Leonard Flom, patented Bruch's idea. Their belief that one can identify people based on individual iris features was supported by their clinical experience. However, they were unable to develop such a process.

In 1989 John Daugman [2], a Harvard mathematician, constructed algorithms for iris recognition upon request of A. Safir and L. Flom. These algorithms, patented by Daugman in 1994, form the basis for all basic iris recognition systems and products currently being used. The first commercial products became available in 1995 [3]. Nowadays companies in several countries are using such variety of products [2], for example, IBM; IrisGuard, Inc.; Securimetrics, Inc.; Panasonic; London Heathrow Airport; and Amsterdam Schiphol Airport.

Moreover, the idea of using iris in biometrics is also popular in science-fiction movies. We should mention the scene in *Demolition Man* (1993), where a bad character played by Wesley Snipes used gouged eye to gain access through a security door, and other movies like *Angels and Demons* (2000) and *The Simpsons Movie* (2007).

As we observe, the field of iris recognition is relatively young, and therefore one may hope for much progress in this field.

### 3.2 Human and Computer Vision

This chapter will start with an introduction about human vision. You may ask why, why human vision and what it would do with computer vision. What benefits will the computer engineers have from having this knowledge? The answer is that actually whenever we deal with a natural concept or a real event, we should always study it from inside before going further with the automatic process. The physical nature of the eye and the medical knowledge about it will give the engineer wide understanding about its iris. Researchers study the iris from computer vision point of view, but they always need to check what may affect their results. The iris has an exceptional pattern with trillions of shape and texture distribution combinations. And it is this fact that makes it one of the most reliable biometric features to distinguish between people.

The reliance on iris in biometric identification based on wide range of advantages of this human body characteristic [4]. Table 3.1 contains comparisons among biometric identifiers on the seven criteria, which can represent their basic properties – iris achieved good results in this comparison. Iris pattern and structure evidence is long-term – structural formation that is fixed about 1 year in age. It is an internal organ that is well protected against damage and worn by a highly

**Table 3.1** Comparisons among biometrics based on different factors – high (H), medium (M), low (L) [5]

Biometric identifier	Universality	Distinctiveness	Permanence	Collectability	Performance	Acceptability	Circumvention
DNA	H	H	H	L	H	L	L
Face	H	L	M	H	L	H	H
Fingerprint	M	H	H	M	H	M	M
Hand geometry	M	M	M	H	M	M	M
Iris	H	H	H	M	H	L	L
Keystroke	L	L	L	M	L	M	M
Signature	L	L	L	H	L	H	H
Voice	M	L	L	M	L	H	H

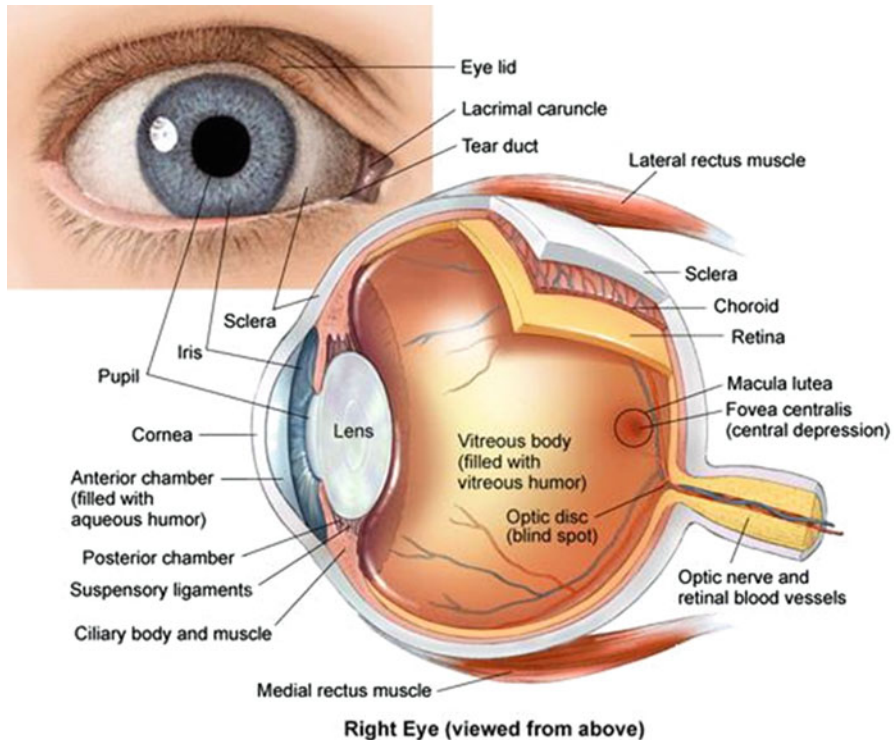


Fig. 3.1 Eye anatomy [6]

transparent and sensitive membrane (the cornea, see Fig. 3.1). The iris is mostly flat, and its geometric configuration is only controlled by two complementary muscles that control the diameter of the pupil. This makes the iris shape far more predictable than, for instance, that of the face. An iris scan is similar to taking a photograph and can be performed from about 10 cm to a few meters away [7]. Moreover, the identification speed through iris scanning is very fast and cannot be compared with that of any other technology.

Additional important medical facts about the iris are the following:

- Every iris is different, even left and right or between identical twins.
- It is worn by easy to damage the iris by external factors, because of its deep location and because iris is worn by the cornea.
- Iris does not change during the whole life unless there is a disease or a mechanical damage.
- It is naturally destroyed few seconds after death.
- The physiological reaction of the iris toward the light and thenatural movement of the pupil make it impossible to replace the iris tissue with a photograph, by spoofers, for example.

Usually, the problems of the eye reflect on its iris shape, pattern, and texture – simply what affects its information code that it has behind its structure and construction. Therefore, in order to study what affects the success rate of iris classification and recognition, researchers should study the iris nature. They should know these and other environmental conditions and geometrical changes (with the light effects as their main factor). Any disturbance in the pattern information the iris supplies the automatic machines with is of importance and worth studying. This is because every single defect that hits the iris and makes its shape or pattern changed/deformed would affect the results.

Considering all this information, the authors found it of great importance and benefit to introduce the problems with iris automatic recognition, particularly those of medical type and nature. With these concerns, the chapter will present first the medical effects. Then the geometrical factors and the other changes that may also affect the iris pattern will be given.

### 3.3 Iris Anatomy

The iris arises from the anterior portion of the eye ciliary body. It divides the space between the cornea and lens into anterior and posterior chambers. It contains variable amounts of pigment:

- Heavy pigmentation in the anterior layer results in brown eyes.
- If pigment is limited to the posterior layer, the iris appears blue or gray because light refracts within the unpigmented anterior layer. The iris contains primitive myoepithelial cells surrounding central aperture, the pupil [8].

#### 3.3.1 *The General Structure of the Iris*

There are two layers building the iris: stroma – the front pigmented fibrovascular tissue – and, below the stroma, the pigmented epithelial cells.

The stroma adheres to the sphincter pupil which contracts it in a circular motion and a dilator which pulls the iris radially to extend the pupil, pulling it in folds – alike the camera shutter. The iris is divided into two major parts: pupillary and ciliary zone.

#### 3.3.2 *Histological Features*

The first layer of the iris, from front to back, is anterior limiting layer. The second one is the stroma. The sphincter and dilator muscles are next. Then anterior pigment myoepithelium and posterior pigment epithelium close the structure of the iris.

Iris is a very important element of human vision. It is kind of a camera shutter, which is automatically regulated. It is responsible for controlling the size of the

pupil and the amount of light reaching the retina; on the other hand it cuts circles of dispersal because of the imperfection of the optical system of the eye.

### 3.4 Iris Pathology and Diseases

This section will be shown in a table. It will contain full information about the iris diseases that affect its shape and pattern, or at least it may disturb the information collected from the iris. Table 3.2 will give information about such diseases – their names with a short description to show what exactly it does to cause a defect. A full eye image with the iris defect shown in it is given.

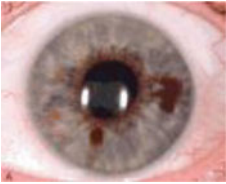


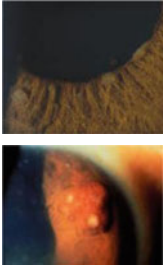
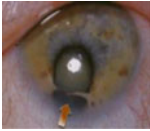
### 3.5 Iris Recognition Process: A Review of Selected Existing Algorithms

The automatic iris scanning systems make use of the visible features of the iris. After taking iris scan, a unique entry in the database is created. Thanks to this, for individual verification the person is required to look at an equipped camera that scans and verifies the iris in a few seconds.

The process of capturing an iris and projecting it into a biometric template is made up of three major steps:

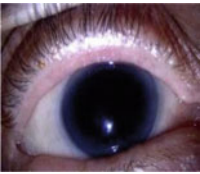

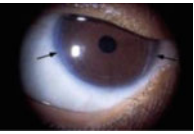

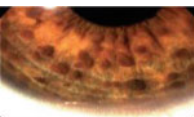

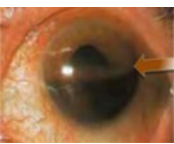
- Capturing the image – one of the main challenges of automated iris recognition is to capture a high-quality image to include as many features of the iris as possible. The image should have sufficient resolution and sharpness, high contrast ratio, etc. The system should eliminate artifacts. Images are generally acquired in near infrared illumination. The distance between the eye and the camera can vary between 4 and 50 cm. There is an iris recognition system which works at a distance of about 3 m [18]. Iris diameter needs typically about 100–200 pixels for the extraction of good texture.
- Localizing the iris and optimizing its image – an iris recognition algorithm first has to identify the approximately concentric circular outer boundaries of the iris and the pupil in a photo of an eye. One has often to deal with additional problems caused by the eyelids which can reduce the surface of the iris. To deal with these problems along with the iris template, the mask template is also formed which makes sure that the noisy or less significant parts of the image are not encoded. Sensitivity to a wide range of edge contrast and insensitivity to irregular borders are the desired characteristics of localization algorithms.
- Storing and comparing of the images – the set of pixels covering the iris is transformed into a bit pattern that preserves the information essential for a comparison between two irises. To perform authentication, which includes identification or verification, an iris template is compared to stored template values in a database.

**Table 3.2** Iris diseases – names, images, and defect description

Disease		Eye image	Description
1.	Melanocytic tumors	(a) Nevus 	Nevus is a benign tumor. It can involve any portion of the iris, and it is mainly flat. An iris nevus rarely can lead to an irregular pupil. This would cause some changes in the iris structure and hence its pattern [9]
	Melanoma	(b) 	An iris melanoma is a malignant tumor. It usually concerns elder people, mostly with bright irises and occurs unilaterally. An iris melanoma is an elevated and variable pigmented neoplasm. Melanoma most often is larger than an iris nevus and can induce an irregular pupil [9]
2. Iritis	(a) Nongranulomatous		Hypopyon (arrow) – level of exudative fluid covers a part of the iris [10]
	(b) Granulomatous		Koeppe nodules appear at the pupil margin and changes iris structure [11] Busacca nodules on the periphery of the iris [12]
3. Iris defects	(a) Coloboma iridis		Congenital absence in the low part of the iris. It destroys part of the iris [10]

(continued)

**Table 3.2** (continued)

Disease	Eye image	Description
(b) Aniridia		Congenital absence of the iris – it occurs bilaterally [13]
4. Glaucoma (a) Rubeosis iridis		New abnormal blood vessels, known as neovascularization, on the surface of the iris. This is caused by hypoxia, which involves retina. This happens when there is a lack of blood in the area, for example, in diabetic retinopathy [14]
(b) Axenfeld-Rieger syndrome (a defect that affects teeth, eyes, and abdomen, characterized by three types, but only two of them affect the iris)		Axenfeld syndrome – the most typical feature of the eye is a posterior embryotoxon and prominent Schwalbe's line (arrows) [15]
		Rieger syndrome – it contains hypoplasia of the iris stroma, displacement of the pupil, and full-thickness colobomas of the iris [16]
(c) Von Recklinghausen disease (Neurofibromatosis type I)		Iris pattern destroyed by Lisch nodules (nodular changes in the iris shape) [17]
		Congenital ectropion uvulae – it means the iris pigment epithelium is on the anterior surface of the iris [12]
5. Hyphema		Blood in anterior chamber. It is usually caused by a mechanical eye injury. Arrow shows the iris blood coverage [10]



Many methods have been developed for automatic iris recognition [19, 20]; they can be divided due to their feature encoding algorithms:

- The Gabor wavelet approach by Daugman [21]
- The Laplacian parameter approach by Wildes [22]
- Zero-crossings of the wavelet transform at various resolution levels by Boles et al. [23]
- The independent component analysis approach by Huang et al. [24]
- The texture analysis using multichannel Gabor filtering and wavelet transform by Zhu et al. [25] and many others

However, the existing algorithms are in many cases not successful enough to solve some basic problems. The commercial iris recognition systems usually cannot distinguish between high-quality photograph of a person's face and the real face [26]. And this is a big security problem, for example. To solve this problem, a human may supervise the use of an iris recognition system. Another solution is to track the movement of the eye in order to verify that the iris is alive.

There are free distributed iris image databases on the Internet, for example, the database provided by the Chinese Academy of Sciences' Institute of Automation (CASIA) [27] includes 756 iris images from 108 eyes – images are stored as BMP format with a  $320 \times 280$  resolution.

### 3.6 Daugman's Classical Algorithm

The classical algorithm proposed by John Daugman is the most popular approach to individual identification by iris pattern recognition. The main steps in this algorithm are presented as follows:

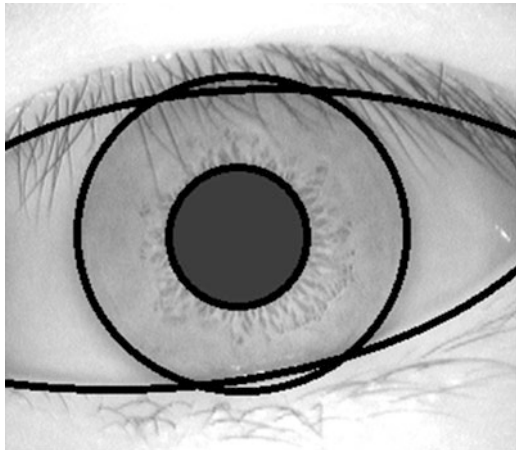
- Iris localization
- Normalization
- Feature encoding
- Matching

#### 3.6.1 Localizing and Segmentation

John Daugman's algorithm uses integrodifferential operator for determining the localization of the circular iris and pupil in addition to the areas of the upper and lower eyelids. The operator is defined as follows:

$$\max_{(r, x_0, y_0)} \left| G_{\sigma}(r) * \frac{\partial}{\partial r} \oint_{r, x_0, y_0} \frac{I(x, y)}{2\pi r} ds \right|,$$

**Fig. 3.2** Example iris localization and segmentation. The area between the *two circles* would define the iris while the arcs define the eyelids edge



where:

$l(x,y)$  – image (containing the eye) pixel color

$G_\sigma(r)$  – the Gaussian smoothing function with scale ( $\sigma$ ) is given by the following formula

$$G_\sigma(r) = \frac{1}{\sqrt{2\pi}\sigma} \exp\left(-\frac{(r-r_0)^2}{2\sigma^2}\right),$$

$r$  – searching radius

$s$  – contour given by circle with  $r, x_0, y_0$  parameters

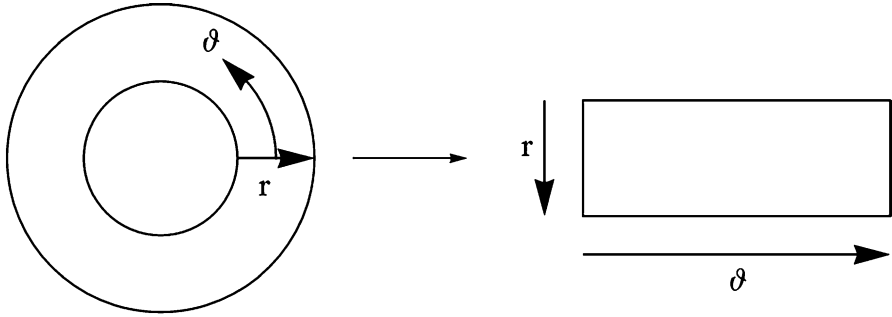
The smoothed image is scanned for a circle that has the maximum gradient change that indicates an edge. To obtain a precise localization, the operator is applied iteratively. During this operation, the smoothing function scale is changed to increase the accuracy. Eyelids are localized in a similar way – the contour  $s$  is changed from a circular into an arc (Fig. 3.2).

This approach uses the first derivative of the image and performs a search to locate geometrical elements at it. However, one has to be careful with using it, because the algorithm uses local scale, so it can perform badly, if the image contains reflection or other types of noise.

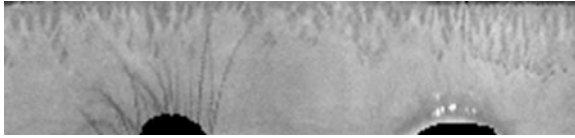
The above method assumes that the iris has a circular boundary; nowadays research shows that we can reject this assumption and give better algorithm for iris segmentation [28].

### 3.6.2 Normalization

Given an iris region, we need to extract a fixed number of features based on this region. We should be able to do this regardless (if possible) of the image resolution.



**Fig. 3.3** Daugman's rubber-sheet model – Daugman normalization model



**Fig. 3.4** Iris after normalization (based on Fig. 3.2)

Hence, we need to transform the given iris region into a fixed reference system. This transformation forms the normalization process; it is achieved by varieties of methods. For example, the Cartesian to polar coordinate transform suggested by J. Daugman converts the region of interest into a rectangular representation introducing an interesting method of normalization (Fig. 3.3).

This way we unfold the frequency information contained in the localized region in order to next simplify the feature extraction (Fig. 3.4).

Daugman's rubber-sheet model of iris normalization can be described as follows: Let  $\theta$  ( $\theta \in [0, 2\pi]$ ) and  $r$  ( $r \in [0, 1]$ ) parameters describe the polar-coordinate system. Then the rubber sheet is modeled as

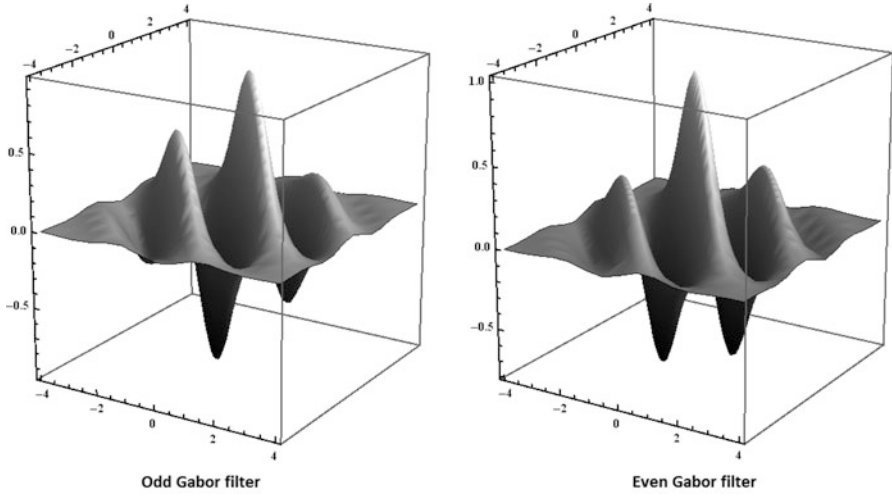
$$I(x(r, \theta), y(r, \theta)) \rightarrow I(r, \theta),$$

where

$$\begin{aligned} x(r, \theta) &= (1 - r)x_p(\theta) + rx_i(\theta) \\ y(r, \theta) &= (1 - r)y_p(\theta) + ry_i(\theta) \end{aligned}$$

where  $r_p$  and  $r_i$  are, respectively, the radii of the pupil and the iris, while  $(x_p(\theta), y_p(\theta))$  and  $(x_i(\theta), y_i(\theta))$  are the coordinates of the pupillary and limbic boundaries in the direction  $\theta$ .

This model introduces the normalized nonconcentric polar representation of the iris, which is size and translation invariant. It should be noted that the previous steps have a big influence on this stage, which in particular implies that the wrong recognition of the center or the radius of the iris can have profound consequences.



**Fig. 3.5** Odd and even Gabor filter

### 3.6.3 Feature Encoding

It has been shown by Oppenheim and Lim [29] that phase information rather than amplitude information provides the most significant information within an image. Taking only the phase will allow encoding of discriminating information in the iris while discarding the redundant information such as illumination, which is represented by the amplitude component. Therefore, it is required to transform the iris feature points into a domain where phase information is available. We need a domain where we have information about localization of pixels and frequency changing, with good ability of local measurement – that is why we use Gabor filters.

Gabor filters (Fig. 3.5) are the products of a Gaussian filter with oriented complex sinusoids. They come in pairs (decomposition of a signal is accomplished using a quadrature pair of Gabor filters), each consisting of a symmetric filter (a cosine modulated by a Gaussian)

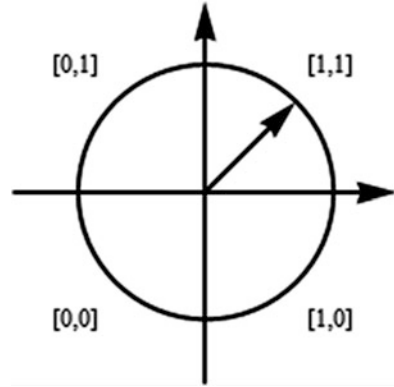
$$G_S(x, y) = \cos(k_x x + k_y y) \exp\left(-\frac{x^2 + y^2}{2\sigma^2}\right)$$

and antisymmetric filter (a sine modulated by a Gaussian)

$$G_A(x, y) = \sin(k_x x + k_y y) \exp\left(-\frac{x^2 + y^2}{2\sigma^2}\right),$$

where  $(k_x, k_y)$  determines the spatial frequency and the orientation of the filter and  $\sigma$  determines the scale of the filter. A filter bank is formed by varying the frequency,

**Fig. 3.6** The quantization of the phase information into four levels



the scale, and the filter orientation. The center frequency of the filter is specified by the frequency of the sine/cosine waves, while the bandwidth of the filter is specified by the width of the Gaussian.

Daugman's algorithm uses two-dimensional version of Gabor filters in order to encode iris pattern data:

$$h_{\{\text{Re}, \text{Im}\}}(r, \theta) = \text{sgn}_{\{\text{Re}, \text{Im}\}} \int_{\rho} \int_{\phi} I(\rho, \phi) e^{-i\omega(\theta-\phi)} e^{-\frac{(r-\rho)^2}{\alpha^2}} e^{-\frac{(\theta-\phi)^2}{\beta^2}} \rho d\rho d\phi$$

where

- $h_{\{\text{Re}, \text{Im}\}}(r, \theta)$  is the iris code at a feature point (iris feature) with  $r$  to be its distance from the pupil boundary and  $\theta$  angle from the horizontal axis
- $I(\rho, \theta)$  is the raw iris image in the dimensionless coordinate system
- $\alpha, \beta$  is the width of the Gaussians used in modulation

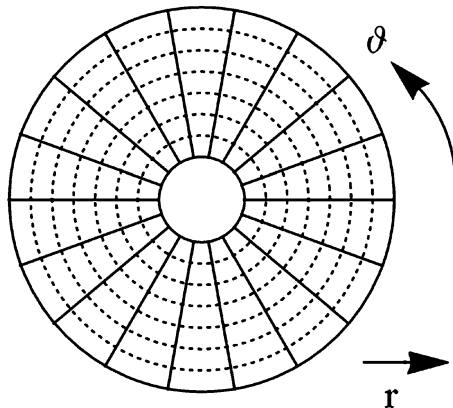
Daugman demodulates the output of Gabor filters in order to compress the data. This is done by quantizing the phase information into four levels, for each possible quadrant in the complex plane (Fig. 3.6).

In fact the iris region (after normalization) is divided into  $8 \times 128$  sectors, and then for each we apply Gabor filters (Fig. 3.7). Hence, as an outcome we obtain 2,048 bits of code which can be understood as a compressed representation of the current iris features – this is what we commonly understand by **IrisCode**.

### 3.6.4 Verification and Identification Methods

For image feature matching, the Hamming distance is chosen as a metric for recognition. The Hamming distance is calculated using only the bits generated from the true iris region – the calculations do not take into account the nonessential parts of the iris. **The modified Hamming distance formula is given as**

**Fig. 3.7** Iris divided into sectors



$$HD = \frac{\|(codeA \oplus codeB) \cap maskA \cap maskB\|}{\|maskA \cap maskB\|}$$

where *codeA* and *codeB* are two bit-wise templates to compare and *maskA* and *maskB* are the corresponding noise masks. Masks allow to deal with iris surface distortion, such as presented in Table 3.2, light reflections, visible eyelashes, etc.

In theory, Hamming distance of two iris templates generated from the same iris image equals 0. However, since the normalization is not perfect, this will usually not occur in practice. We commonly obtain noise that goes undetected, and hence, a nonzero difference will usually appear.

The method proposed by Daugman corrects the misalignment in the normalized iris pattern. In order to cope with rotational inconsistencies, when the Hamming distance of two templates is calculated, one template is shifted to one bit left and right. This operation is interpreted as a rotation of a specific angle of the input image. Then the Hamming-distance values are calculated. This bit offset in the horizontal direction corresponds to the starting area of the iris angle indicated by the rubber-sheet model. For the iris distance we choose only the smallest which corresponds to the best match between two templates.

The number of bits transferred during each shift equals two times the number of filters used, since each filter will generate two bits of information from one pixel-normalized region. The real number of changes necessary to normalize rotational inconsistencies will be determined by the maximum angle difference between two pictures of the same eye. One change is defined as one shift to the left and one shift to the right. The example of the shifting process is presented in Fig. 3.8.

In practice the maximum number of shifts is fixed to the left and to the right. This “brute force” rotation-angle estimation is performed with each element of the database causing one of the main disadvantages of this method.

Moreover, in the case of iris recognition under relatively unfavorable conditions, using images acquired at different distances and by different optical platforms, Hamming distance can give wide range of images which can be classified as the same (Fig. 3.9).

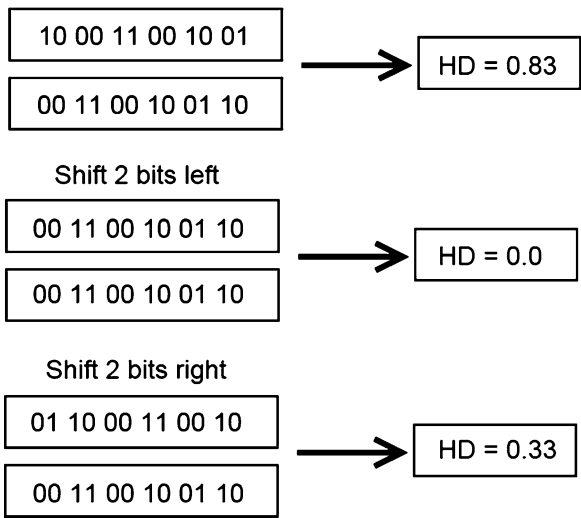


Fig. 3.8 The shifting process for one shift to the left and one to the right

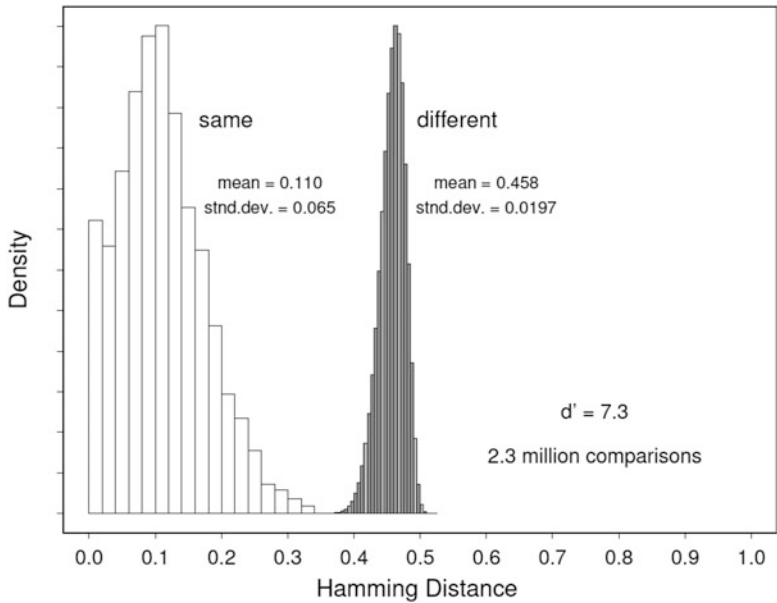


Fig. 3.9 Decision environment for iris recognition [30]

### 3.7 The Modified Fourier Descriptor Method: A New Approach to Rotation Detection in Iris Pattern Recognition

As we have seen, there is a strong need for rotation invariant iris recognition methods. This task can be obtained by, as classically, rotating by a fixed angle the iris pattern as can be seen, for example, in [31]. Another more advanced approach is applied in [32] where the use of directionlets (wavelets specialized in representation of elongated and oriented features along edges or contours) is used.

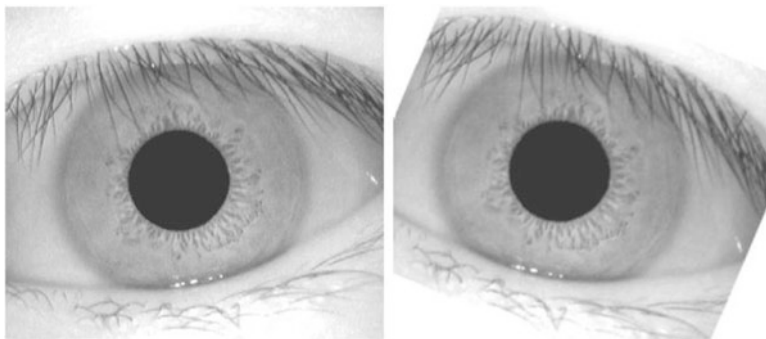
In this section we present another different approach (a method worked out by the first author) for recovering the angle in the iris images using some modification to the classical Fourier descriptor method [33]. An example of such images is shown in Fig. 3.10.

The classical Fourier descriptor method applied is not suitable for the case of iris pattern recognition because the iris is represented as concentric circles – the rotation of circles cannot be recovered basing on the rotation of the edges (Fig. 3.11). Moreover, the difference in illumination in various photographs can cause errors in edge detection.

To deal with such inconveniences we propose the following procedure:

#### 3.7.1 Algorithmic Idea

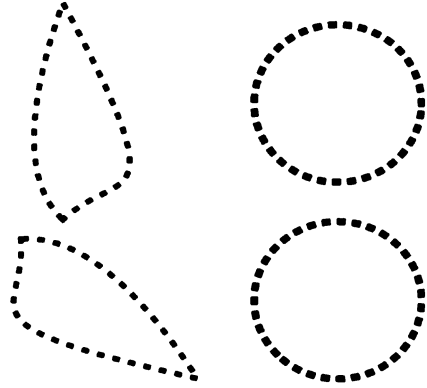
Assume that we already applied classical Daugman's algorithm. After normalization with rubber-sheet model, two normalized iris images  $I_{Org}$  and  $I_{Rot}$  are obtained for original and rotated images, respectively. We can reduce our investigations to images in gray scale where each pixel is coded by a number from the set  $\{0, \dots, 255\}$ . Afterward, in order to reduce complexity of calculations, resize the images, for example, set the new size to  $8 \times 256$ (image height  $\times$  width). In this case an angle recover accuracy error of  $360/256 \approx 1.5$ degree is obtained.



**Fig. 3.10** Iris images: original (non-rotated) and rotated



**Fig. 3.11** Example of two shapes with digital boundary. The rotation of the second does not allow to estimate the angle of rotation



Now, the following two matrices are dealt with

$$\begin{aligned}\tilde{I}_{Org} &= \left( c_{kn}^{Org} \right)_{k,n} \in M_{8 \times 256}(Z), \\ \tilde{I}_{Rot} &= \left( c_{kn}^{Rot} \right)_{k,n} \in M_{8 \times 256}(Z)\end{aligned}$$

where  $c_{kn}^{Org}$  and  $c_{kn}^{Rot}$  are integer numbers for  $k \in \{0, \dots, 7\}$  and  $n \in \{0, \dots, 255\}$ .

Next construct the vectors of features describing  $\tilde{I}_{Org}$  and  $\tilde{I}_{Rot}$  by Fourier descriptors which allow to compare both images.

Calculate the first Fourier descriptor

$$\begin{aligned}C_{k1}^{Org} &= \frac{1}{16} \sum_{n=0}^{255} c_{kn}^{Org} \exp\left(-i \frac{\pi n}{128}\right), \quad k = 0, \dots, 7 \text{ and} \\ C_{k1}^{Rot} &= \frac{1}{16} \sum_{n=0}^{255} c_{kn}^{Rot} \exp\left(-i \frac{\pi n}{128}\right), \quad k = 0, \dots, 7,\end{aligned}$$

where  $k$  changes for each row of these matrices.

Denote

$$\begin{aligned}x_{Org} &= \left( C_{0,1}^{Org}, \dots, C_{7,1}^{Org} \right), \text{ and} \\ x_{Rot} &= \left( C_{0,1}^{Rot}, \dots, C_{7,1}^{Rot} \right).\end{aligned}$$

It is easy to see, by properties of Fourier transform, that those vectors are in the form  $x_{Rot} = e^{i\varphi} v$  and  $x_{Org} = w$ , for some  $v, w \in \mathbb{C}^8$ .

### 3.7.1.1 Remark

We can look at our problem from the mathematical point of view and formulate it as follows:

Let nontrivial vectors  $v, w \in C^n$  be fixed. Define a function  $f$  as follows:

$$f_{v,w} : [0, 2\pi] \ni \varphi \rightarrow \|e^{i\varphi}v - w\|^2 \in R_+.$$

To solve the problem of estimating rotation angle, we have to find the minimum of this function – it describes the rotation one of the vectors relatively to the second one; the optimum is reached when vectors are reduced to the same one-dimensional linear subspace. This will reduce the difference between them. It is easy to calculate that the minimum of the function  $f$  is obtained for

$$\varphi = \text{Arg} \frac{\overline{\langle v, w \rangle}}{|\langle v, w \rangle|}.$$

Based on this, we get

$$\varphi = \text{Arg} \frac{\overline{\langle x_{Org}, x_{Rot} \rangle}}{|\langle x_{Org}, x_{Rot} \rangle|} \quad (3.1)$$

where  $\varphi$  is the desired angle. Thus, we obtain a closed formula for the rotation angle (3.1), which gives us an advantage in terms of computation speed.

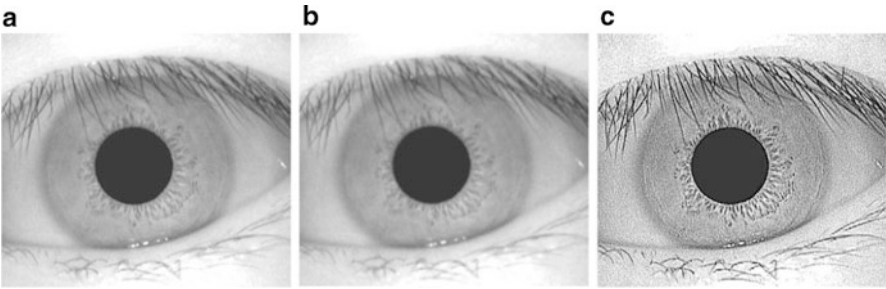
The formula used in (3.1) is also somewhat reminiscent of the widely used spectral angle mapper (SAM) [34, 35], which measures the angle between the spectral vector  $r = (r_1, r_2, \dots, r_L)^T$  and  $s = (s_1, s_2, \dots, s_L)^T$ . It is given by

$$SAM(r, s) = \cos^{-1} \left( \frac{\langle r, s \rangle}{\|r\|_2 \times \|s\|_2} \right).$$

Summarizing, the new rotation angle-estimation algorithm can be stated as follows:

### 3.7.2 Algorithm

1. Perform Daugman's rubber-sheet model standardization for  $I_{Org}$  and  $I_{Rot}$ .
2. Determine the second Fourier descriptor from each rubber row and construct the vectors  $x_{Org}$  and  $x_{Rot}$ .
3. Estimate the angle of rotation using (3.1).
4. Compare irises by Hamming distance using the estimated angle.



**Fig. 3.12** Iris image modification: (a) original image, (b) blurring, (c) sharpening

**Table 3.3** Angle detection in different image modifications (angle in degrees)

		Algorithm results			
Method	Angle	Classical approach		Authors' Fourier-based approach	
		Recognized	Error	Recognized	Error
None	5	5.00	0.00	4.22	0.78
Blur		0.00	5.00	3.69	1.31
Sharpen		0.00	5.00	3.66	1.34
None	23	23.00	0.00	22.50	0.50
Blur		3.00	20.00	21.87	1.73
Sharpen		0.00	23.00	23.10	0.10

The above algorithm was tested by comparing the efficiency with the classical shifting method. The images were noised by performing standard “destructive” operation on images (Fig. 3.12) such as brightness correction, contract reduction, gamma correction, blurring, and sharpening. Table 3.3 contains comparison of recovered angle between the classical and the proposed Fourier transform–based method.

The error level in both examples suggests that the new method is less affected by the proposed image modifications then the classical one.

Obviously, one can also apply other approaches to translation-, rotation-, illumination- and scale-invariant iris recognition systems [36].

### 3.8 Other Alternatives

As mentioned before, there still are other approaches for automatic iris recognition. The most important and widely used is Wildes [22] system, which was developed at Sarnoff Labs. There are some advantages to Wildes’ design. This system has a less-intrusive light source designed to eliminate specular reflections. Moreover it can be more stable to noise perturbations.

The Wildes et al. algorithm performs localization and segmentation in two steps [37]. Firstly, the image is converted into edge map – we extract information about

the edge points in the image. One possible method to do this is thresholding the magnitude of the image intensity gradient considering smoothed image. We can alternatively use various other methods in this step, for example, Roberts Cross, Sobel, or Canny [33].

Second step allows us to select circles describing, for example, pupil using voting procedure on parametric definitions of the iris boundary contours, which can be realized via Hough transforms [38]. Hough transform can be described in following steps:

- Find all the desired (edge) feature points in an image – by applying edge detection we can produce a set of boundary descriptions.
- Transform each feature point into a set of parameters – we find the space parameter, from which feature points are obtained as local maxima.
- The transformed feature point “votes” in the parametric space – for each point we calculate the most appropriate parameters describing desire object.
- The votes are accumulated and the local maxima are extracted – we choose the most likely object, the one on which most of the points chose.

Basic idea behind this transform is to transform the pattern detection problem into a parametric space and perform the easier pattern detection problem (e.g., peak detection) in the parametric space. There are a number of problems with the Hough transform method. The most important issue is that it requires threshold values to be chosen for edge detection, and this may result in critical edge points being removed, resulting in failure to detect circles/arcs (Fig. 3.13).

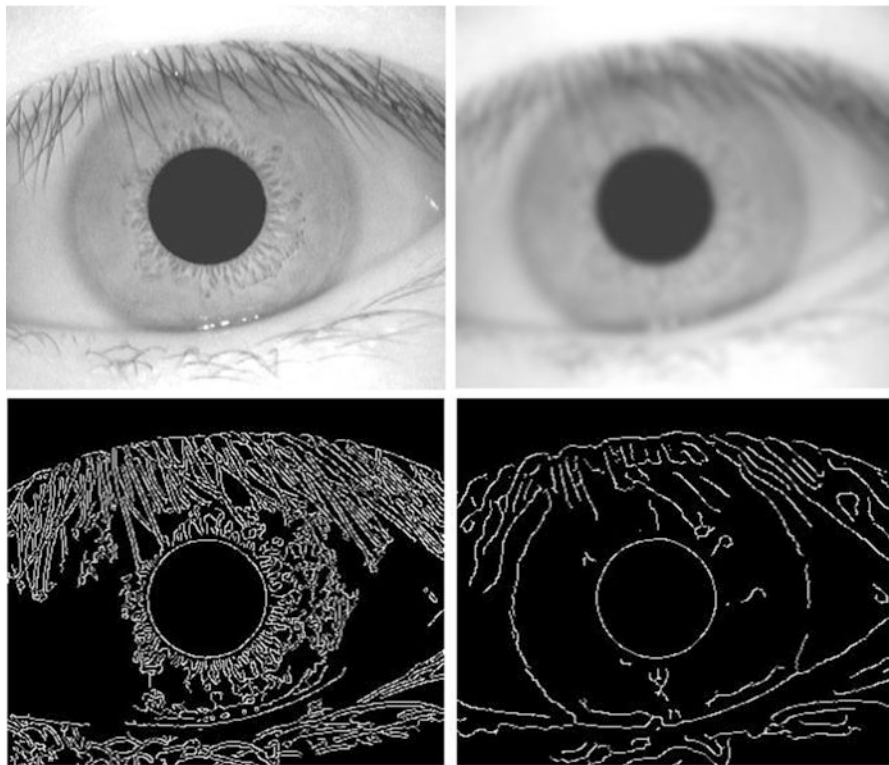
Hough Transform is also employed by Kong and Zhang [39], Tisse et al. [40], Ma et al. [41].

The Wildes et al. system uses an image-registration technique to compensate for both scaling and rotation [22]. The acquired image is rotated and scaled to obtain minimal differences with original image. For feature encoding, we use an isotropic bandpass decomposition derived from application of Laplacian of Gaussian filters to decompose the image data. Next, we represent image as a Laplacian pyramid which is able to compress data – details can be found in [42].

Proper verification and identification is based on normalized correlation between the acquired image and database template. This allows to account for local variations in image intensity that corrupt the standard correlation calculation.

### 3.9 Conclusions

The iris identification and verification process is complex, and the construction of a reliable automatic system requires addressing a number of problems. The chapter presents one of the most popular algorithms developed by John Daugman in detail. Moreover, a new method is applied to recover iris rotation detection. The algorithm is based on Fourier descriptor analysis of normalized iris images. The numerical experiments show that the authors’ algorithm is better than classical Daugman



**Fig. 3.13** Edge-map for two images: original (*on left*) and blurred (*on right*)

“brute force” approaches. Furthermore, it is relatively insensitive to rotation, contrast modification, illumination-level modification, blurring, and sharpening of the acquired input iris images. The last part of this chapter contains a brief knowledge about Wildes’ algorithm concept for iris recognition – the most popular alternative for Daugman approach.

**Acknowledgment** This work was partially supported by AGH University of Science and Technology in Cracow, grant no. 11.11.220.01.

## References

1. Bertillon A (1885) La couleur de l’iris. Rev Sci 36(5):65–73
2. John Daugman’s webpage, Cambridge University, Faculty of Computer Science & Technology, Cambridge. <http://www.cl.cam.ac.uk/~jgd1000/>. Accessed 28 May 2012
3. Iridian Technologies: about Iridian. In: Historical timeline. <http://www.iriscan.com/about.php?page=4>. Accessed 28 May 2012
4. Iris ID – Iris Recognition Technology. <http://www.irisid.com>. Accessed 28 May 2012

5. Jain AK, Ross A, Prabhakar S (2004) An introduction to biometric recognition. *IEEE Trans Circuits Syst Video Technol* 14(1):4–20
6. BioGraphix. <http://www.biriaographixmedia.com/human/eye-anatomy.html>. Accessed 28 May 2012
7. Stamp M, Wiley J (2006) Information security: principles and practice. Wiley Online Library, Hoboken, NJ
8. April E (1997) Clinical anatomy. Williams and Wilkins, Baltimore
9. Tasman W, Jaeger EA (2007) Duane's clinical ophthalmology. Williams and Wilkins, Philadelphia
10. Medscape reference. In: Drugs, diseases and procedures, image no. 3, 6, and 13. <http://reference.medscape.com/features/slideshow/iris-changes>. Accessed 28 May 2012
11. London NJS, Cunningham ET (2012) Prompt and aggressive treatment might have preserved this mechanic's vision. [http://www.aao.org/publications/eyenet/200804/am\\_rounds.cfm](http://www.aao.org/publications/eyenet/200804/am_rounds.cfm). Accessed 28 May 2012
12. Shiuey Y (2012) General ophthalmology quiz 6, Digital Journal of Ophthalmology – knowledge review. [http://www.djo.harvard.edu/site.php?url=/physicians/kr/459&page=KR\\_AN](http://www.djo.harvard.edu/site.php?url=/physicians/kr/459&page=KR_AN). Accessed 28 May 2012
13. Digital reference of ophthalmology, review, Columbia University, New York. At: <http://dro.hs.columbia.edu>
14. Fulk G (2012) Ocular disease I: glaucoma, uveitis and lens disorders, photo no. 38, Northeastern State University. <http://arapaho.nsuok.edu>. Accessed 28 May 2012
15. Children network – disease research and education network, fig. 3. <http://childrennetwork.org/physicians/ags.html>. Accessed 28 May 2012
16. Jonathan T (2012) A systemic problem, Bascom Palmer Eye Institute Grand Rounds. <http://media.med.miami.edu>. Accessed 28 May 2012
17. Cackett P, Vallance J, Bennett H (2005) Neurofibromatosis type 1 presenting with Horner's syndrome. *Nat Eye* 19:351–353. doi:10.1038/sj.eye.6701478, Published online. Available (19.04.2012) at: <http://www.nature.com/>
18. Dong W, Sun Z, Tan T (2009) A design of iris recognition system at a distance. In: Chinese conference on pattern recognition 4–6 November 2009, Nanjing, China, (CCPR 2009). <http://avss2012.org/2009papers/gjhy/gh99.pdf>. Accessed 21 September 2012
19. Masek L (2003) Recognition of human iris patterns for biometric identification. Master's thesis, University of Western Australia
20. Farag AA, Elhabian SY (2012) Iris recognition. <http://www.cvip.uofl.edu/wwwcvip/education/ECE523/Iris%20Biometrics.pdf>. Accessed 28 May 2012
21. Daugman J (1993) High confidence visual recognition of persons by a test of statistical independence. *IEEE Trans Pattern Anal Mach Intell* 15(11):1148–1161
22. Wildes RP (1997) Iris recognition: an emerging biometric technology. *Proc IEEE* 85(9):1348–1363
23. Boles W, Boashash B (1998) A human identification technique using images of the iris and wavelet transform. *IEEE Trans Signal Process* 46(4):1185–1188
24. Huang YP, Luo SW, Chen EY (2002) An efficient iris recognition system. In: Proceedings of 2002 international conference on machine learning and cybernetics, 4–5 November 2002, Beijing, China, vol 1, pp 450–454
25. Zhu Y, Tan T, Wang Y (2000) Biometric personal identification based on iris patterns. In: Proceedings of 15th international conference on pattern recognition, 3–7 September 2000, Barcelona, Spain, vol 2, pp 801–804. <http://www.cbsr.ia.ac.cn/publications/yzhu/Bio-metric%20Personal%20Identification%20Based%20on%20Iris%20Patterns.pdf>. Accessed 21 September 2012
26. Harowitz S (2007) Faking fingerprints and eying solutions. *Secur Manage Mag*
27. Center for Biometrics and Security Research. <http://www.cbsr.ia.ac.cn>. Accessed 28 May 2012

28. Daugman J (2007) New methods in iris recognition. *IEEE Trans Syst Man Cybern B: Cybernetics* 37(5):1167–1175
29. Oppenheim AV, Lim JS (1981) The importance of phase in signals. *Proc IEEE* 69(5):529–541
30. Daugman J (2004) How iris recognition works. *IEEE Trans Circuits Syst Video Technol* 14(1):21–30
31. Takano H, Nakamura K (2009) Rotation independent iris recognition by the rotation spreading neural network. In: *IEEE 13th international symposium on consumer electronics*, 25–28 May 2009, Kyoto, Japan. ISCE'09, pp 651–654
32. Velisavljevic V (2009) Low-complexity iris coding and recognition based on directionlets. *IEEE Trans Inf Forensics Secur* 4(3):410–417
33. Gonzalez RC, Woods RE (2002) *Digital image processing*. Prentice Hall, Upper Saddle River
34. Du Y, Chang CI, Ren H, Chang CC, Jensen JO, D'Amico FM (2004) New hyperspectral discrimination measure for spectral characterization. *Opt Eng* 43:1777
35. Chang CI (2003) *Hyperspectral imaging: techniques for spectral detection and classification*. Springer, New York
36. Du Y, Ives RW, Etter DM, Welch TB (2006) Use of one-dimensional iris signatures to rank iris pattern similarities. *Opt Eng* 45:037201
37. Wildes RP, Asmuth JC, Green GL, Hsu SC, Kolczynski RJ, Matey JR, McBride SE (1994) A system for automated iris recognition. In: *Proceedings of the second IEEE workshop on applications of computer vision*, 5–7 December 1994, Sarasota, FL, USA pp 121–128
38. Illingworth J, Kittler J (1988) A survey of the Hough transform. *Comput Vision Graph Image Process* 44(1):87–116
39. Kong WK, Zhang D (2001) Accurate iris segmentation based on novel reflection and eyelash detection model. In: *Proceedings of 2001 international symposium on Intelligent multimedia, video and speech processing*, 2–4 May 2001, Hong Kong, China pp 263–266. <http://www3.ntu.edu.sg/home/AdamsKong/publication/ISIM.pdf>. Accessed 21 September 2012
40. Tisse C, Martin L, Torres L, Robert M (2002) Person identification technique using human iris recognition. In: *Proceedings of vision interface*, pp 294–299. <http://citeseerx.ist.psu.edu/viewdoc/download?doi=10.1.1.5.3.130&rep=rep1&type=pdf>. Accessed 21 September 2012
41. Ma L, Wang Y, Tan T (2002) Iris recognition using circular symmetric filters. In: *Proceedings of 16th international conference on pattern recognition*, 11–15 August 2002, Quebec City, QC, Canada vol 2, pp 414–417. [http://hci.iwr.uni-heidelberg.de/publications/dip/2002/ICPR2002/DATA/05\\_2\\_25.PDF](http://hci.iwr.uni-heidelberg.de/publications/dip/2002/ICPR2002/DATA/05_2_25.PDF). Accessed 21 September 2012
42. Burt P, Adelson E (1983) The Laplacian pyramid as a compact image code. *IEEE Trans Commun* 31(4):532–540